Discovery and epitypification of the sexual stage of Cadophora fallopiae on Fallopia spp. in Japan.

Hiyori Itagaki (✉ itagaki@kahaku.go.jp)

National Museum of Nature and Science: Kokuritsu Kagaku Hakubutsukan   https://orcid.org/0000-0001-8678-0826

Tsuyoshi Hosoya

National Museum of Nature and Science: Kokuritsu Kagaku Hakubutsukan

Abstract

The genus *Cadophora* was established as a dematiaceous asexual fungi characterized by solitary phialides with distinct collarettes, and phylogenetically suggested to be the asexual stage of the family *Pyrenopezizaceae* (*Helotiales*, Ascomycetes). However, the sexual stage is unknown except in a few species. *Cadophora fallopiae* which occurs on the overwintered stems of *Fallopia* in Europe, has only been described for its conidiomatous asexual stage. In Japan, *C. fallopiae*-like conidiomata were discovered associated with the apothecia of *Pyrenopeziza* sp. on the same substrate (the stem of *Fallopia* spp). Therefore, conspecificities of the apothecia and conidiomata were suspected. A detailed comparison of morphology and ITS-5.8S sequences confirmed that this fungus is identical to *C. fallopiae* known in Europe, and that the sexual stage was connected with its asexual stage for the first time. Based on the genetic diversity of single ascosporous isolates derived from a single apothecium, we hypothesized that the reason the sexual stage has not been discovered in Europe is the lack of a compatible mating type.

Introduction

The genus *Cadophora* Lagerb. & Melin 1927 was established with *C. fastigiata* as a type species (Lagerberg et al. 1927). Most species of *Cadophora* are dematiaceous asexual fungi that produce solitary phialides with distinct pale to hyaline collarettes. Due to thier similar phialide morphology, *Cadophora* was once synonymized with *Phialophora* Medlar (Conant 1937) (currently, *Phialophora* is placed in the order *Chaetothyriales* M.E. Barr). Later, Gams (2000) reinstated *Cadophora* and incorporated species morphologically similar to the asexual stage of *Mollisia* and its allies.

Ecologically, members of *Cadophora* normally have multiple trophic modes, and are found in extremely diverse habitats, including soil, plant residues, living plants, seawater, and marine glaciers (Mandyam and Jumpponen 2005; Navarrete et al. 2011mä et al. 2017; Nagano et al. 2017; Durán et al. 2019; Maciá-Vicente et al. 2020; Zhang et al. 2022). Root-inhabiting *Cadophora* are characterized by melanized hyphae in plant tissues and known as dark septate endophytes (DSEs) (Jumpponen and Trappe 1998; Sieber 2002, 2007; Addy et al. 2005), which affect host plant growth or provide tolerance to environmental stress (Mandyam and Jumpponen 2005). Several species of *Cadophora* are also commonly known as important pathogens in agriculture causing stem rot of soybean (Allington and Chamberlain 1948) and wood decay of cultivated fruits (Di Marco and Osti 2008; Gramaje et al. 2011; Travadon et al. 2015).

Phylogenetic analysis based on multi-gene sequences revealed that *Cadophora* belongs to the family *Pyrenopezizaceae*, and its close relationships with sexual genera, such as *Pirottaea* Sacc. and *Pyrenopeziza* Fuckel, have been suggested (Harrington and McNew 2003; Carmody et al. 2020; Ekanayaka et al. 2019). DNA-based analyses have also resulted in the incorporation of other fungi into *Cadophora* [*C. orchidicola* (Sigler & Currah) M.J. Day & Currah (formerly *Leptodontidium orchidicola* Sigler & Currah)] or their transfer to other genera [*Coniochaeta lignicola* (Nannf.) Z.U. Khan (= *Cadophora*

lignicola (Nannf.) J.F.H. Beyma) and *Hyaloscypha finlandica* (C.J.K. Wang & H.E. Wilcox) Vohník, Fehrer & Réblová (= *Cadophora finlandica* (C.J.K. Wang & H.E. Wilcox) T.C. Harr. & McNew)].

Presently, 48 epithets in *Cadophora* are listed in Index Fungorm (https://www.indexfungorum.org/ as of August 8, 2023); however, the known sexual stages are limited. All sexual stages are similar to those of mollisioid fungi (e.g. *Cadophora dextrinospora* (Korf) Koukol & Maciá-Vicente and *C. lacriformis* Ekanayaka & K. D. Hyde. The latter has not yet found an asexual stage) (Greenleaf and Korf 1980; Ekanayaka et al. 2019; Maciá-Vicente et al. 2020).

Maciá-Vicente et al. (2020) indicated that some *Cadophora* species have an asexual stage that is quite different from the original morphological circumscription of the genus. For example, *C. orchidicola* (Sigler & Currah) M.J. Day & Currah produces indehiscent conidia on undifferentiated hyphae or slightly swollen conidiogenous cells (Currah et al. 1987). *Cadophora antarctica* Rodr.-Andr., Stchigel, Mac Corm. & Cano, *C. fascicularis* Koukol & Maciá-Vicente, and *C. variabilis* Koukol & Maciá-Vicente produce two types of conidia (acropetal chains of ramoconidia and holoblastic conidia) (Crous et al. 2017; Maciá-Vicente et al. 2020). *Cadophora obovata* Koukol & Maciá-Vicente produces putatively monoblastic conidiogenous cells (Maciá-Vicente et al. 2020). *Cadophora echinata* Koukol & Maciá-Vicente, *C. gamsii* Koukol & Maciá-Vicente, and *C. inflata* Q.M. Wang, B.Q. Zhang & M.M. Wang form chains or microsclerotia-like inflated cells (Maciá-Vicente et al. 2020; Zhang et al. 2022).

Cadophora fallopiae Crous & Akulov is a species with multiform morphological characteristics, and has only been described as a conidiomatous asexual stage with conidiophores lined along the internal cavity of the conidioma and sympodially producing conidiogenous cells (Crous et al. 2020). *Cadophora fallopiae* is found from the overwintered stems of *Fallopia japonica* (Houtt.) Ronse Decr. in Germany, and *F. sachalinensis* (F. Schmidt) Ronse Decr. in Poland (Crous et al. 2020). Crous et al. (2020) classified this fungus in *Cadophora* by phylogenetic analysis based on the partial 28S nuclear ribosomal large subunit rRNA gene.

In Japan, an undescribed mollisioid fungus circumscribed in *Pyrenopeziza* was found from the overwintered stems of *Fallopia* spp. Conidiomata were also discovered near the apothecia of this fungus, and their morphology was very similar to *C. fallopiae*. Therefore, we suspected conspecificity of this undescribed *Pyrenopeziza* sp. and conidiomata. The objective of this study was to elucidate the relationship between *Pyrenopeziza* sp. and conidiomata by a detailed comparison of morphology and internal transcribed spacer (ITS) sequences and to reconsider the genus-level classification based on phylogenetic relationships with *C. fallopiae* and other related genera. We also hypothesized that the sexual stage has not been discovered in Europe, based on the possible mating system elucidated by the genetic diversity of single ascosporous isolates derived from an apothecium.

Material and Methods

Sample collection and isolation

Multiple specimens of *Pyrenopeziza*-like apothecia from *Fallopia* were collected from spring to early summer (May to July) in Hokkaido and high-altitude areas of Honshu (altitude of 1,598 m at Mt. Amari in Yamanashi Pref. and 1,320 m at the Sugadaira Research Station in Nagano Pref.) following the occurrence of apothecia on the stems of *F. japonica* and *F. sachalinensis* that accumulated on damp, shaded ground (Table 1). Isolates were obtained from fresh apothecia by discharging ascospores on a potato dextrose agar (PDA; Nissui, Tokyo, Japan), according to the procedure described by Itagaki et al. (2019).

Voucher specimens were dried at 60 ºC overnight and deposited in the mycological herbarium of the National Museum of Nature and Science (TNS; specimens were numbered with a prefix TNS-F-). The isolates were also deposited at the Biological Resource Center, National Institute of Technology and Evaluation (NBRC). For a detailed analysis of genetic diversity, 20 single ascospores and conidia were isolated from one of the apothecia (TNS-F-86753) and conidioma (TNS-F-86412), respectively, using Skerman's micromanipulator (Skerman 1968).

To induce the asexual stage under culture, mycelia derived from ascosporous isolates were cut from the developed colony on PDA slants and inoculated on 9 cm Petri dishes containing synthetic low-nutrient agar (SNA without filter paper: KH_2PO_4 1 g, KNO_3 1 g, $MgSO_4 \cdot 7H_2O$ 0.5 g, KCl 0.5 g, glucose 0.2 g, sucrose 0.2 g, agar 15 g, and water 1 L,) (Gerlach and Nirenberg 1982), cornmeal agar (CMA; Nissui), and PDA. The inoculated plates were sealed with Parafilm and incubated for 2−3 months at 20 ºC under black light (FL15BLB, peak wavelength 352 nm, Toshiba, Tokyo, Japan).

Morphological observations

The overall appearance of the apothecia was observed under a stereomicroscope (SZ61; Olympus, Tokyo, Japan) and photographed with a digital camera (DS-L4, Olympus). The colonies on PDA were photographed using a digital camera (D40; Nikon Inc., Tokyo, Japan). To observe the pigment dissolution and discoloration of the apothecia in potassium hydroxide (KOH) solution, the apothecia were immersed in 3% KOH droplets and observed under a stereomicroscope. To observe the microstructures of the apothecium (such as asci, ascospores, and paraphyses), hyphal, and conidia-producing structures, fungal structures were picked from the substrates or colonies, mounted in cotton blue in lactic acid (CB/LA) or water on a slide glass, and gently squashed with a cover glass. Cross-sections of the rehydrated apothecium and fresh conidioma were prepared using a freezing microtome, as described by Itagaki et al. (2019). These sections were examined under an optical microscope (Olympus BX51 microscope equipped with Nomarski phase interference; Olympus) and photographed using a digital camera (DS-L3; Nikon).

The lengths and widths of 20 ascospores and asci were measured in CB/LA preparations using an ocular micrometer. Measurements of ascospores, asci, and paraphyses were performed using rehydrated specimens. The mean ± standard deviation of each measured value with outliers is shown in parentheses. Illustrations were prepared using line-drawing attachments (U-DA; Olympus). The colors of the apothecia and colonies were described by citing the codes in the CMYK system using a color chart

(DIC Corp., Tokyo). Morphological observations of apothecium microstructures were conducted using both dried and fresh materials.

DNA extraction, PCR, and sequencing

DNA extraction and ITS sequencing were conducted as described by Itagaki et al. (2019). To examine the conspecificity of the Japanese specimens and *C. fallopiae* (including the holotype and paratype), an ITS sequence identity matrix was generated using BioEdit ver. 7.0.5.2 (Hall 1999).

To check the polymorphisms within RPB2, sequences were obtained from each DNA sample extracted from single-ascosporous isolates using the forward primer RPB2-6F (5'−TGG GGK WTG GTY TGY CCT GC−3') and reverse primer RPB2-7R (5'−CCC ATW GCY TGC TTM CCC AT−3') (Liu et al. 1999). PCR and sequencing were carried out under the same program used for ITS analysis. The aligned sequences were observed using BioEdit, and different nucleotides within ITS and RPB2 were manually inspected.

Taxon sampling

In TNS, nine specimens (including the specimens collected in this study) with high ITS sequence similarity (≥ 98.5%) to TNS-F-86411 were available. ITS sequences of *C. fallopiae* [including ex-holotype culture, CPC 38013 (CBS 146083)] and other species belonging to the following genera currently classified in *Pyrenopezizaceae* by Baral (2016) and Wijayawardene et al. (2020) were obtained from GenBank: *Cadophora*, *Collembolispora* Marvan ová & Pascoal, *Dennisiodiscus* Svrček, *Graphium* Corda, *Helgardiomyces* Crous, *Mastigosporium* Riess, *Neospermospora* Crous & U. Braun, *Oculimacula* Crous & W. Gams, *Pirottaea* Sacc., *Pyrenopeziza*, *Rhexocercosporidium* U. Braun, *Rhynchobrunnera* B.A. McDonald, U. Braun & Crous, *Rhynchosporium* Heinsen ex A.B. Frank, *Spermospora* R. Sprague, *Ypsilina* J. Webster, Descals & Marvanová (Table 1). As the outgroup, *Mollisia* cf. *cinerea* (DAOMC 252029) and *Phialocephala dimorphospora* W.B. Kendr. (ex-type culture, CBS 200.62) in *Mollisiaceae* were selected.

Phylogenetic analysis

The sequences were aligned using MAFFT v. 7 (Katoh and Standley 2013). The resulting alignments were divided into ITS1, 5.8S, and ITS2, and all insertions/deletions were manually deleted using BioEdit. To evaluate the phylogenetic relationships among the sampled taxa, a phylogenetic analysis of the ITS sequence was conducted using Ultrafast Maximum Likelihood (IQ-Tree) and Bayesian inference (MrBayes). The automatic substitution model setting, 1,000 ultrafast bootstrap (BS) replications, and the Shimodaira-Hasegawa approximate likelihood ratio test (SH-aLRT) with 1,000 replicates were conducted using ModelFinder (Anisimova et al. 2011; Kalyaanamoorthy et al. 2017) under the Bayesian information criterion (BIC) for ML. The most suitable substitution model for the divided ITS sequences was estimated using Kakusan4 (Tanabe 2011) based on the corrected BIC (Schwarz 1978) for Bayesian inference and the Akaike information criterion (AICc) (Sugiura 1978) for ML analysis.

The ML tree was constructed using IQ-Tree (Nguyen et al. 2015) based on the suitable substitution models TIM2e + G4 for ITS1, K2P + G4 for 5.8S, and TIM3e + R2 for ITS2. Bayesian phylogenetic analysis was performed using MrBayes v. 3.2.7 (Ronquist et al. 2012) with substitution models containing the

BIC4 parameter (proportional models ITS1 and ITS2 for SYM + Gamma and K80 + Gamma for 5.8S). Two independent Markov chain Monte Carlo (MCMC) chains were run for four million generations, and every 1,000 generations were sampled. After each run, Tracer v.1.6 (Rambaut et al. 2014) was used to verify that the standard deviation of split frequencies (ASDSF) was less than 0.01 and the estimated sample size of all parameters was over 100 as an indication of convergence. The first 25% of the trees were discarded as burn-in, and the remaining trees were used to construct a consensus tree with a 50% majority-rule and determine the Bayesian posterior probabilities (BPP) for individual branches. The consensus trees were visualized using FigTree v. 1.4.4 (Rambaut 2018). Branches with SH-aLRT ≥ 80%, ultrafast BS ≥ 95%, and BPP ≥ 0.95 were regarded as strongly supported.

Results and Discussion

Morphological and genetic comparison

The collected fungus showed typical characteristics of the genus *Pyrenopeziza*, such as erumpent apothecia (Figs. 1A, B), ectal excipulum consisting of brown-walled textura angularis (Fig. 1H), margin composed of elongated, colorless cells (Figs. 1D, 3A), and paraphyses lacking reflective vacuoles (Fig. 1K) (Gremmen 1958; Baral 1992; Nauta and Spooner 1999c; Baral 2016).

The coexistence of asexual structure (conidiomata) and apothecia was observed on the same substrate (Fig. 2A), and the asexual stage is described as follows: Conidiomata spherical, 150–500 µm diam., with moderately developed parietal tissue, without ostioles, and subepidermal to erumpent; vertical section of conidiomata showing a wall composed of 3–5 layers of pale brown cells (5–15 µm across) with dark brown hyphae interwoven at the base (Fig. 2E). Conidiophores short, hyaline, arising around the cavity of the conidioma (Figs. 2C, E). Conidiogenous cells inconspicuous, subcylindrical, hyaline, branching sympodially, and 5–15(18) × 1.5–2.5(3.5) µm (Figs. 2F, 3E). Conidia acicular-filiform to subcylindrical, hyaline, straight to slightly curved, aseptate, (7)10–55 × 1.5–2 µm, gelatinous, released by a crack of parietal tissue (Fig. 2D), becoming waxy when dried. These morphologies and measurements of the conidia-producing structures agreed well with the original description of *C. fallopiae* (Crous et al. 2020).

Crous et al. (2020) observed the immature and infertile conidiomata of *C. fallopiae* and a cladophialophora-like asexual stage on SNA. The conidiophores arose directly from the superficial hyphae of the colony, and the conidia are similar in morphology to the conidia produced in the field, except that they were disarticulated at the septa into phragmospores (Crous et al. 2020). However, in this study, mature and fertile conidiomata were successfully induced in ascosporous isolates on CMA and SNA, with abundant conidial production (Fig. 2B). Most conidia were aseptate in both the field and culture. No morphological differences in conidia and sympodial conidia-producing structure between those in the culture and those in the field, except for the width of the conidia (slightly wider in culture, up to 3 µm).

The ITS sequence similarities among the isolates from *Pyrenopeziza*-like apothecia, conidia (TNS-F-86412), and *C. fallopiae* (CPC 38011, 38013, and 35742) were 98.8–100%. Based on morphological and genetic comparisons, the conidiomata collected in Japan were identified as *C. fallopiae*, and their correlation with *Pyrenopeziza*-like sexual stage was confirmed.

Taxonomy

To add the sexual stage to *C. fallopiae*, we choose TNS-F-86411 as an epitype according to International Code of Nomenclature for Algae, Fungi, and Plants (McNeill et al. 2012). Below we provide the description for the sexual stage.

Cadophora fallopiae Crous & Akulov, Fungal Systematics and Evolution 6: 180. 2020.

MycoBank: MB835069

Epitype

TNS-F-86411, Sugadaira Montane Research Center, Ueda City, Nagano Pref., JAPAN, 5 June 2021, on overwintered stems of *F. japonica*; culture ex-epitype NBRC 115372 (= FC-8871).

Apothecia scattered to gregarious, sessile, subglobose then cup-shaped under epidermis when immature, erumpent and saucer-shaped when mature, subepidermal when dried, 0.1–0.25 mm high; disc entire to sinuate, 0.3–1.5 mm diam., dark grey (K40–70) or olive grey (C0M0Y10–40K60) when fresh, shrunk and turned darker when dried; margin pruinose with elongated hairs, white. *Ectal excipulum* textura globulosa to angularis at basal receptacle, becoming textura prismatica at the upper flank, 50–60 µm thick at base, 20–40 µm thick at the upper flank, without crystals or exudates, composed of thick-walled cells, entirely dark gray (K60–80); cortical cells polylateral, 5–15 µm across, smooth, thick-walled, dark brown; marginal hair (15)21–35(40) × 2.5–3 µm, cylindrical clavate with blunt head, smooth, thin-walled, hyaline. *Medullary excipulum* textura prismatica, 35–80 µm thick, hyaline. *Asci* (35)46–60(65) × 5–7.5 µm, cylindrical clavate, 8-spored, base arising from croziers, with apical pore amyloid in Melzer's solution with 3% KOH pretreatment. *Ascospores* (6.5)8–10(12.5) × 2–2.5 µm, ellipsoid to fusiform with obtuse to subacute extremes, sometimes contain 2–3 small guttles, thin-walled, aseptate, hyaline. *Paraphyses* filiform, straight to waving, smooth, rarely branching at base, 1–3 septate below, thin-walled, hyaline, tip cells not containing refractive vacuoles in fresh mounted on water.

Colony of NBRC 115372 on PDA with entire margin, flat to slightly convex at the center with aerial hyphae, dense, cottony to velvety, beige (C10–20M20Y20K10) to dark grey (K50–70), white to pale grey (K10–20) at the edge, darker from the reverse, with indistinct sectors, without soluble pigment and crystals. Chlamydospore-like cells in the aerial hyphae of the colony after two months, dark brown, lobe-shaped to irregular, solitary or in 2–3 series of cells, smooth, containing several oil globules in the cytoplasm. Clumps of cells attached to the bottom of the Petri dish containing CMA, dark brown, thick-

walled, scallop-shaped to irregular, 10–30 μm across, solitary to aggregated, smooth, and containing several oil globules.

Additional specimens examined: TNS-F-16835 (FC-2357) and 16836 (FC-2347), Sugadaira Research Station, Ueda City, Nagano Pref., 10 June 2007; TNS-F-86044 (FC-8547), Sugadaira Research Station, Ueda City, Nagano Pref., 22 June 2018; TNS-F-86112 [NBRC 115363 (= FC-8614, derived from conidia)] and 86130 (FC-8613), Morappu Campsite, Chitose City, Hokkaido, 19 June 2018; TNS-F-86197 (FC-8671), Sugadaira Research Station, Ueda City, Nagano Pref., 8 June 2019; TNS-F-86411 (FC-8871) and 86412 (FC-8872), Sugadaira Research Station, Ueda City, Nagano Pref., 5 June 2021; TNS-F-86413 (FC-8873), Mt. Amari, Asahi Town, Nirasaki City, Yamanashi Pref., 14 June 202; TNS-F-86753 (FC-9202), Sugadaira Research Station, Ueda City, Nagano Pref., 31 May 2022; TNS-F-86764 (FC-9213), Obora, Sugadaira plateau, Ueda City, Nagano Pref., 1 July 2022, on overwintered stem of *F. japonica*.

Notes: In addition to a detailed morphological description of the sexual stage, chlamydospore-like cells (Figs. 1L, 3F) and clumps of cells similar to appressoria were newly observed (Figs. 2M, 3G). Both structures were abundantly formed in poor-nutrient agar (SNA and CMA).

Phylogenetic analysis

Molecular phylogenetic analyses were performed based on 98 ITS sequences (Table 1). In the ML analysis, a best-scored tree was yielded with loglikelihood − 2590.607. In the Bayesian phylogenetic analysis, a 50% majority rule consensus tree was constructed based on the remaining 3,000 trees. Because no topological conflict occurred between the phylogenetic trees of ML and Bayesian analyses, only the ML tree is shown (Fig. 4).

ITS-based Phylogenetic analysis showed that the TNS specimens and *C. fallopiae* (CPC 38011, 38013, and 35742) formed a single cluster with high support; hence, no speciation trend between the Japanese and European specimens was observed (Fig. 4). The ITS phylogeny generated many heterogeneous clades with weak support within the lineage. A few genera, such as *Rhynchobrunnera*, *Rhyncosporium*, and *Mastigosporium* were strongly supported. However, many genera, including *Cadophora* and *Pyrenopeziza* were polyphyletic and dispersed throughout the lineage. *Pyrenopeziza revincta* (P. Karst.) Gremmen (ARON3150.P) was positioned in the outgroup apart from the type species of *Pyrenopeziza*, *P. chailletii* (Pers.) Fuckel. Some *Cadophora* species, including the type species *C. fastigiata*, tended to form a large clade with weak support at the base of *Pyrenopezizaceae*, reconstructing a robust phylogenetic tree inferred from multiple genes is desirable. Because the phylogenetic relationship between *C. fallopiae* and other genera was not revealed, any taxonomic treatment of *C. fallopiae* was withheld.

Multi-gene phylogenetic analysis of *Cadophora* species conducted by Zhang et al. (2022) showed that the genus was divided into two clades: one contained most of *Cadophora* species (including the type, *C. fastigiata*) with phialidic asexual stage (referred to as "*Cadophora* s. str."). The other group included the rest of *Cadophora* species (including *C. fallopia*) with multiform conidiogenesis and members of other asexual genera in *Pyrenopezizaceae*. A comprehensive phylogenetic analysis based on multiple genes

would reveal the proper position of *Cadophora* species with multiform asexual stages in *Pyrenopezizaceae*.

Possibility of immigration from Japan to Europe with Fallopia spp.

While *Fallopia* spp. are important pioneering and traditional plants in Japan, *F. japonica*, in particular, is recognized as one of the worst invasive alien plants on European and global scales (Nentwig et al. 2018; Lowe et al. 2000). After the introduction of female *F. japonica* from Japan to Europe by Phillip von Siebold in the early 19th century (Bailey 2012), *F. japonica* rapidly expanded its distribution and seriously impacted local biodiversity and ecosystems (Gerber et al. 2008). Therefore, new approaches for the biological control of *F. japonica* using parasitic arthropods and pathogenic fungi are urgently required (Kurose et al. 2006; Djeddour and Shaw 2011). Further examinations are needed to reveal the biological interaction between *C. fallopiae* and *Fallopia* spp., but the high host specificity and presence of appressorium-like cells (Figs. 1M, 3G) of *C. fallopiae* suggest that this fungus may inhabit living *Fallopia* spp. as an endophyte or pathogen. The strong host specificity of saprophyte suggests a potential endophytic lifestyle as part of its lifecycle (Itagaki and Hosoya, 2021).

In Japan, both the sexual and asexual stages of *C. fallopiae* have been found on the same substrate during the same season, whereas only the asexual stage has been reported in Europe (Crous et al. 2020). The absence of apothecia in European specimens can be explained by the hypothesis that *C. fallopiae* is heterothallic and that only one mating type has been introduced from Japan to Europe with the host plant, resulting in asexual reproduction. The heterothallism of *C. fallopiae* distributed in Japan was strongly suggested in this study because genetic polymorphisms were found from 19 single-spored isolates from a single apothecium (Table 2). Six and two haplotypes were detected in RPB2 and ITS, respectively. This genetic diversity indicated that *C. fallopiae* is not homothallic, suggesting *C. fallopiae* has a complex mating system. However, details of this mating system require further investigation.

The absence of sexual stage for several years after its introduction has been reported in several heterothallic pathogenic fungi, such as *Phytophthora infestans* (Mont.) de Bary in Japan (Akino et al. 2005), powdery mildew in Europe (Yarwood 1957; Seko et al. 2008; Gross et al. 2021), and *Ophiostoma novo-ulmi* (Buisman) Nannfeldt in Europe (Paoletti et al. 2006). If *C. fallopiae* is heterothallic, and both mating types have already been introduced, mating and/or apothecia formation may be inhibited by environmental factors. Future studies are expected to characterize the mating types locus of *C. fallopiae* and its geographic origin and migration routes.

Declarations

Acknowledgements

Conflict of interest

The authors have declared that no competing interests exist.

Author contributions

All authors contributed to this work. H. Itagaki collected, isolated, and observed all specimens used in this study and drafted the original manuscript. T. Hosoya supervised the conduct of this study and reviewed and revised the manuscript draft.

References

1. Addy HD, Piercey MM, Currah RS (2005) Microfungal endophytes in roots. Can J Bot 83:1–13. https://doi.org/10.1139/b04-171

2. Akino S, Kato M, Gotoh K, Naito S, Ogoshi A (2005) Genetic relationships between the dominant genotypes of *Phytophthora infestans* in Hokkaido, Japan. J Gen Plant Pathol 71:200–203. https://doi.org/10.1007/s10327-005-0187-2

3. Allington WB, Chamberlain DW (1948) Brown stem rot of soybean. Phytopathology 23:793–802

4. Anisimova M, Gil M, Dufayard JF, Dessimoz C, Gascuel O (2011) Survey of Branch Support Methods Demonstrates Accuracy, Power, and Robustness of Fast Likelihood-based Approximation Schemes. Syst Biol 60:685–699

5. Bailey J (2012) The Japanese knotweed invasion viewed as a vast unintentional hybridization experiment. Heredity 110:105–110. https://doi.org/10.1038/hdy.2012.98

6. Baral HO (1992) Vital versus herbarium taxonomy: morphological differences between living and dead cells of ascomycetes, and their taxonomic implications. Mycotaxon 44:333–390

7. Baral HO (2016) Inoperculate discomycetes. pp. 157–205. In: Jaklitsch W, Baral HO, Lücking R, Lumbsch T (eds) Syllabus of Plant Families: Adolf Engler's Syllabus der Pflanzenfamilien. Part 1/2 Ascomycota (13th ed. by Frey W). Borntraeger Science Publishers

8. Carmody SM, King KM, Ocamb CM, Fraaije BA, West JS et al (2020) A phylogenetically distinct lineage of *Pyrenopeziza brassicae* associated with chlorotic leaf spot of *Brassicaceae* in North America. Plant Pathol 69:518–537. https://doi.org/10.1111/ppa.13137

9. Conant NF (1937) The occurrence of a human pathogenic fungus as a saprophyte in nature. Mycologia 29:597–598. https://doi.org/10.1080/00275514.1937.12017229

10. Crous PW, Wingfield MJ, Burgess TI, Carnegie AJ, Hardy GSJ et al (2017) Fungal Planet description sheets: 625–715. Persoonia - Molecular Phylogeny and Evolution of Fungi 39:270–467. https://doi.org/10.3767/persoonia.2017.39.11

11. Crous PW, Wingfield MJ, Schumacher RK, Akulov A, Bulgakov TS et al (2020) New and Interesting Fungi. 3. Fungal Systematics and Evolution, 6: 157–231. https://doi.org/10.3114/fuse.2020.06.09

12. Currah RS, Sigler L, Hambleton S (1987) New records and new taxa of fungi from mycorrhizae of terrestrial orchids of Alberta. Can J Bot 65:2473–2482. https://doi.org/10.1139/b87-336

13. Di Marco S, Osti F (2008) Foliar symptom expression of wood decay in Actinidia deliciosa in relation to environmental factors. Plant Dis 92:1150–1157. https://doi.org/10.1094/PDIS-92-8-1150

14. Djeddour D, Shaw R (2011) Could knotweed's reign of terror be over? Pesticides News 91:12–13

15. Durán P, Barra PJ, Jorquera MA, Viscardi S, Fernandez C et al (2019) Occurrence of soil fungi in Antarctic pristine environments. Front Bioeng Biotechnol 7:28. https://doi.org/10.3389/fbioe.2019.00028

16. Ekanayaka A, Hyde K, Gentekaki E, McKenzie EHC, Zhao Q et al (2019) Preliminary classification of *Leotiomycetes*. Mycosphere 10:310–489. https://doi.org/10.5943/mycosphere/10/1/7

17. Gams W (2000) *Phialophora* and some similar morphologically little-differentiated anamorphs of divergent ascomycetes. Stud Mycol 45:187–199

18. Gerber E, Krebs C, Murrell C, Moretti M, Rocklin R et al (2008) Exotic invasive knotweeds (*Fallopia* spp.) negatively affect native plant and invertebrate assemblages in European riparian habitats. Biol Conserv 141:646–654. https://doi.org/10.1016/j.biocon.2007.12.009

19. Gerlach W, Nirenberg H (1982) The genus *Fusarium* – a pictorial atlas. Mitteilungen aus der Biologischen Bundesanstalt für Land- und Forstwirtschaft Berlin-Dahlem, 209: 1–406

20. Gramaje D, Mostert L, Armengol J (2011) Characterization of *Cadophora luteo-olivacea* and *C. melinii* isolates obtained from grapevines and environmental samples from grapevine nurseries in Spain. Phytopathologia Mediterranea 50:112–126

21. Greenleaf MA, Korf RP (1980) *Mollisia* in Macaronesia: an exercise in frustration. Mycotaxon 10:459–472

22. Gremmen J (1958) Taxonomal Notes on mollisiaceous Fungi-VI. The genus *Pyrenopeziza*. Fungus, 28: 37–46

23. Gross A, Petitcollin C, Dutech C, Ly B, Massot M et al (2021) Hidden invasion and niche contraction revealed by herbaria specimens in the fungal complex causing oak powdery mildew in Europe. Biol Invasions 23:885–901. https://doi.org/10.1007/s10530-020-02409-z

24. Hall AT (1999) BioEdit: a user-friendly biological sequence alignment editor and analysis program for windows 95/98/NT. Nucleic Acids Symposium Series, 41: 95–98. https://doi.org/10.14601/Phytopathol_Mediterr-14998u1.29

25. Harrington FA, McNew DL (2003) Phylogenetic analysis places the *Phialophora*-like anamorph genus *Cadophora* in the *Helotiales*. Mycotaxon 87:141–151

26. Itagaki H, Nakamura Y, Hosoya T (2019) Two new records of ascomycetes from Japan, *Pyrenopeziza protrusa* and *P. nervicola* (*Helotiales*, *Dermateaceae* sensu lato). Mycoscience, 60: 189–196. https://doi.org/10.1016/j.myc.2019.02.008

27. Itagaki H, Hosoya T (2021) Lifecycle of *Pyrenopeziza protrusa* (*Helotiales*, *Dermateaceae* sensu lato) in *Magnolia obovata* revealed by field observation and molecular quantification. Mycoscience 62:373–381. https://doi.org/10.47371/mycosci.2021.08.001

28. Jumpponen ARI, Trappe JM (1998) Dark-septate endophytes: a review of facultative biotrophic root-colonizing fungi. New Phytol 140:295–310. https://doi.org/10.1046/j.1469-8137.1998.00265.x

29. Kalyaanamoorthy S, Minh B, Wong T, von Haeseler A, Jermiin LS (2017) ModelFinder: fast model selection for accurate phylogenetic estimates. Nat Methods 14:587–589. https://doi.org/10.1038/nmeth.4285

30. Katoh K, Standley DM (2013) MAFFT multiple sequence alignment software version 7: improvements in performance and usability. Mol Biol Evol 30:772–780. https://doi.org/10.1093/molbev/mst010

31. Kirk PM, Cannon PF, Minter DW, Stalpers JA (2008) Dictionary of the fungi, 10th edition. CABI

32. Kurose D, Renals T, Shaw R, Furuya N, Takagi M et al (2006) *Fallopia japonica*, an increasingly intractable weed problem in the UK: can fungal pathogens cut. through this Gordian knot? Mycologist 20:126–129. https://doi.org/:10.1016/j.mycol.2006.07.021

33. Lagerberg T, Lundberg G, Melin E (1927) Biological and practical researches into blueing in pine and spruce. Sven Skogsvardsforen Tidskr 25:145–272

34. Liu YJ, Whelen S, Hall BD (1999) Phylogenetic relationships among ascomycetes: evidence from an RNA polymerase II subunit. Mol Biol Evol 16:1799–1808. https://doi.org/10.1093/oxfordjournals.molbev.a026092

35. Lowe SM, Browne M, Boudjelas S, De Poorter M (2000) 100 of the world's worst invasive alien species: a selection from the global invasive species database. The invasive species specialist group (ISSG) a specialist group of the species survival commission (SSC) of the world conservation union (IUCN)

36. Maciá-Vicente JG, Piepenbring M, Koukol O (2020) Brassicaceous roots as an unexpected diversity hot-spot of helotialean endophytes. IMA Fungus 11:16. https://doi.org/10.1186/s43008-020-00036-w

37. Mandyam K, Jumpponen A (2005) Seeking the elusive function of the root-colonizing dark septate endophytic fungi. Stud Mycol 53:173–189. https://doi.org/10.3114/sim.53.1.173

38. McNeill J, Barrie FR, Buck WR, Demoulin V, Greuter W et al (2012) International Code of Nomenclature for algae, fungi, and plants (Melbourne Code). Regnum Vegetabile 154:1–240

39. Nagano Y, Miura T, Nishi S, Lima AO, Nakayama C et al (2017) Fungal diversity in deep-sea sediments associated with asphalt seeps at the Sao Paulo Plateau. Deep Sea Research Part II

146:59–67. https://doi.org/10.1016/j.dsr2.2017.05.012

40. Nauta MM, Spooner BM (1999) British Dermateaceae: 4A. Dermateoideae Mycologist 13:146–148. https://doi.org/10.1016/S0269-915X(99)80096-2

41. Navarrete F, Abreo E, Martínez S, Bettucci L, Lupo S (2011) Pathogenicity and molecular detection of Uruguayan isolates of *Greeneria uvicola* and *Cadophora luteo-olivacea* associated with grapevine trunk diseases. Phytopathologia Mediterranea 50:166–175. https://doi.org/10.14601/Phytopathol_Mediterr-9188

42. Nentwig W, Bacher S, Kumschick S, Pyšek P, Vilà M (2018) More than 100 worst alien species in Europe. Biol Invasions 20:1611–1621. https://doi.org/10.1007/s10530-017-1651-6

43. Nguyen LT, Schmidt HA, von Haeseler A, Minh BQ (2015) IQ-TREE: a fast and effective stochastic algorithm for estimating maximum-likelihood phylogenies. Mol Biology Evol 32:268–274. https://doi.org/10.1093/molbev/msu300

44. Paoletti M, Buck KW, Brasier CM (2006) Selective acquisition of novel mating type and vegetative incompatibility genes via interspecies gene transfer in the globally invading eukaryote *Ophiostoma novo-ulmi*. Mol Ecol 15:249–262. https://doi.org/10.1111/j.1365-294X.2005.02728.x

45. Rämä T, Hassett B, Bubnova E (2017) Arctic marine fungi: from filaments and flagella to operational taxonomic units and beyond. Bot Mar 60:433–452. https://doi.org/10.1515/bot-2016-0104

46. Rambaut A (2018) FigTree version 1.4.4. http://tree.bio.ed.ac.uk/software/figtree/ (Accessed 2 December, 2022)

47. Rambaut A, Suchard MA, Xie W, Drummond AJ (2014) Tracer 1.6. http://beast.bio.ed.ac.uk/Tracer. (Accessed 2 December, 2022)

48. Ronquist F, Teslenko M, van der Mark P, Ayres DL, Darling A et al (2012) MrBayes 3.2: efficient Bayesian phylogenetic inference and model choice across a large model space. Syst Biol 61:539–542. https://doi.org/10.1093/sysbio/sys029

49. Schwarz G (1978) Estimating the dimension of a model. The Annals of Statistics 6:461–464. https://doi.org/10.1214/aos/1176344136

50. Seko Y, Bolay A, Kiss L, Heluta V, Grigaliunaite B et al (2008) Molecular evidence in support of recent migration of a powdery mildew fungus on *Syringa* spp. into Europe from East Asia. Plant Pathol 57:243–250. https://doi.org/10.1111/j.1365-3059.2007.01775.x

51. Sieber TN (2002) Fungal root endophytes. In: Waisel Y, Eshel A, Kafkafi U (eds) Plant roots: the hidden half. CRC Press, pp 887–917

52. Sieber TN (2007) Endophytic fungi in forest trees: are they mutualists? Fungal Biology Reviews 21:75–89. https://doi.org/10.1016/j.fbr.2007.05.004

53. Skerman VBD (1968) A new type of micromanipulator and microforge. J Gen Microbiol 54:287–297. https://doi.org/10.1099/00221287-54-2-287

54. Sugiura N (1978) Further analysts of the data by akaike's information criterion and the finite corrections. Commun Stat - Theory Methods 7:13–26. https://doi.org/10.1080/03610927808827599

55. Tanabe AS (2011) Kakusan4 and Aminosan: two programs for comparing nonpartitioned, proportional and separate models for combined molecular phylogenetic analyses of multilocus sequence data. Mol Ecol Resour 11:914–921. https://doi.org/10.1111/j.1755-0998.2011.03021.x

56. Travadon R, Lawrence DP, Rooney-Latham S, Gubler WD, Wilcox WF et al (2015) *Cadophora* species associated with wood-decay of grapevine in North America. Fungal Biology 119:53–66. https://doi.org/10.1016/j.funbio.2014.11.002

57. Wijayawardene NN, Hyde KD, Al-Ani LKT, Tedersoo L, Haelewaters D et al (2020) Outline of fungi and fungus-like taxa. Mycosphere 11:1060–1456. https://doi.org/10.5943/mycosphere/11/1/8

58. Yarwood CE (1957) Powdery mildews. Bot Rev 13:235–301

59. Zhang B, Li X, Li G, Wang QM, Wang M (2022) *Cadophora* species from marine glaciers in the Qinghai-Tibet Plateau: an example of unsuspected hidden biodiversity. IMA Fungus 13:15. https://doi.org/10.1186/s43008-022-00102-5

Tables

Table 1 and 2 are available in the Supplementary Files section.

Figures
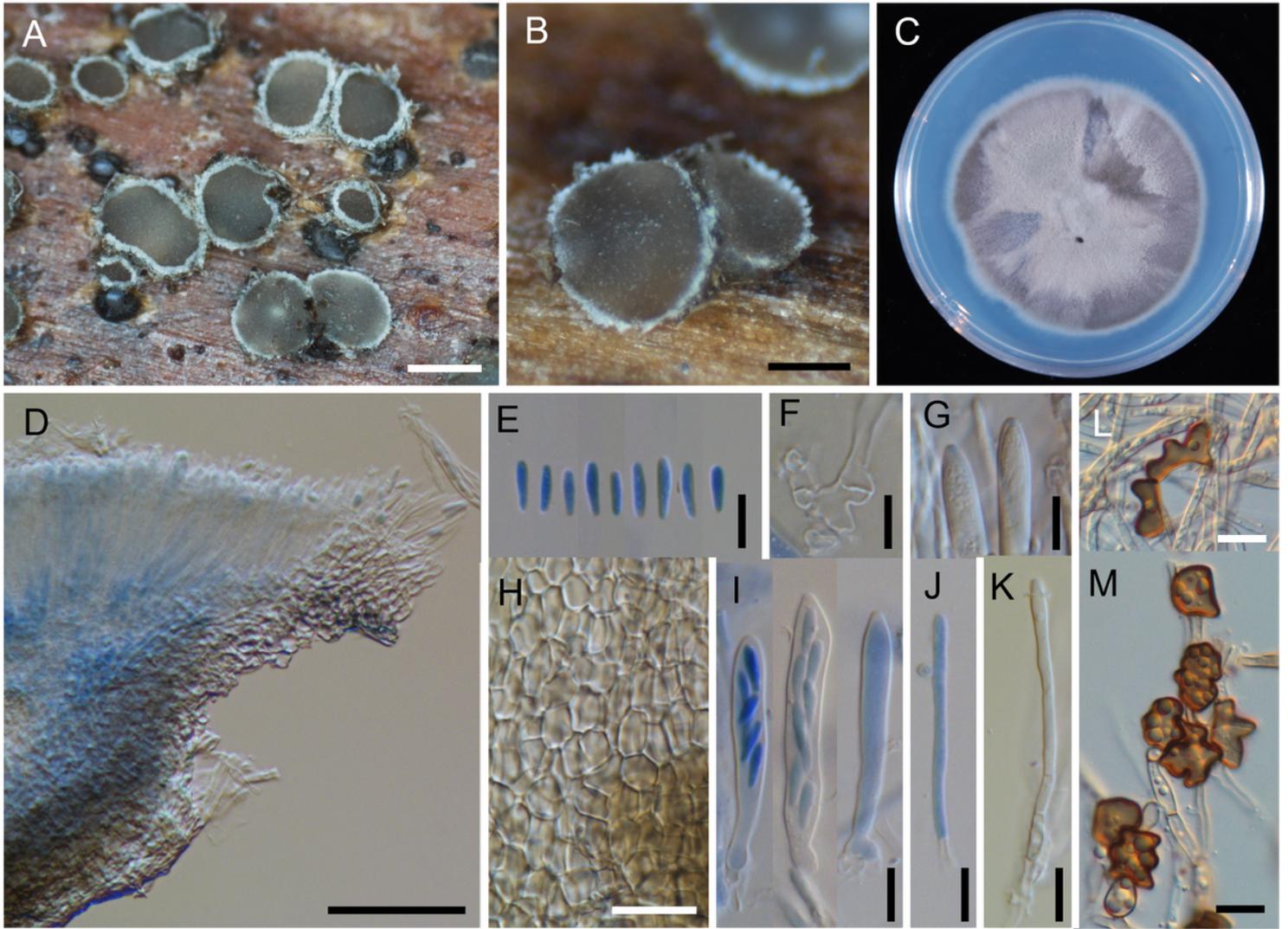
Figure 1

Sexual stage and colony morphology of *Cadophora fallopiae*. **A, B** fresh apothecia on Fallopia japonica (TNS-F-86411). **C** colony derived from multi-spores on PDA (NBRC 115372). **D** vertical section of the apothecium mounted in CB/LA. **E** ascospores mounted in CB/LA. **F** crozier at the base of ascus mounted in LA. **G** blue-stained apical pore of asci with Melzer's reagent after 3% KOH pretreatment. **H** outer most layer of ectal excipulum mounted in LA. **I** asci mounted in CB/LA. **J** paraphysis mounted in CB/LA. **K** fresh paraphysis mounted in water. **L** chlamydospores in aerial hyphae mounted in water. **M** appressorium-like hyphal structures mounted in water. Scale bars: 0.5 mm (**A**); 0.25 mm (**B**); 50 μm (**D**); 20 μm (**H**); 10 μm (**E–G, I–M**).
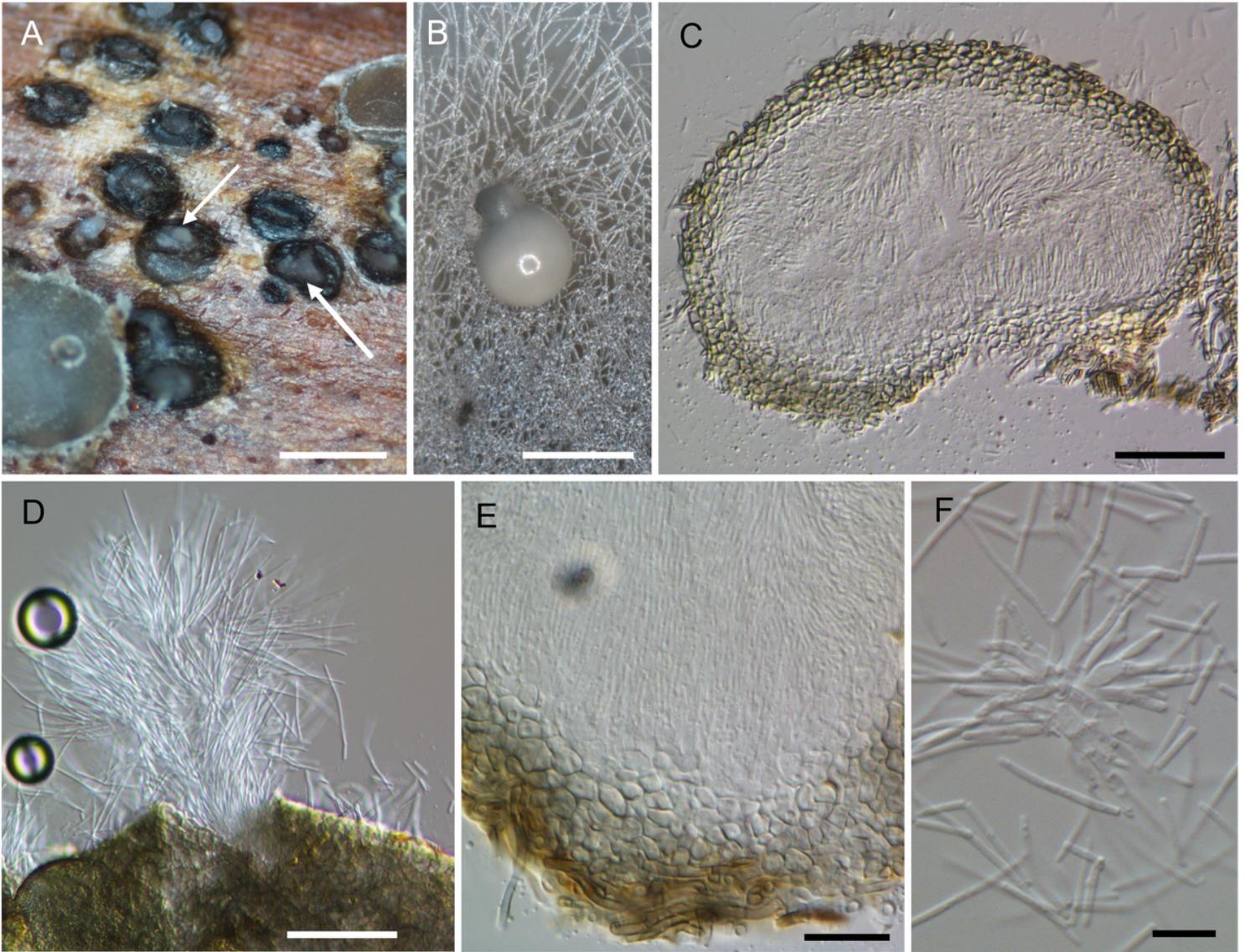
Figure 2

Asexual stage of *Cadophora fallopiae*. **A** conidiomata with conidia (arrows) on *Fallopia japonica*. **B** conidioma produced on CMA. Note that a conidioma covered with opal drop of conidia. **C** vertical section of conidiomata mounted in LA. **D** filamentous conidia released from a crack of conidioma mounted in water. **E** vertical section of basal part of conidioma showing brown hyphae, globose cells, and conidiophores arising around the cavity mounted in LA. **F** conidiophores produced on CMA mounted in LA. Scale bars: 0.5 mm (**A, B**); 50 μm (**C, D**); 20 μm (**E**); 10 μm (**F**).
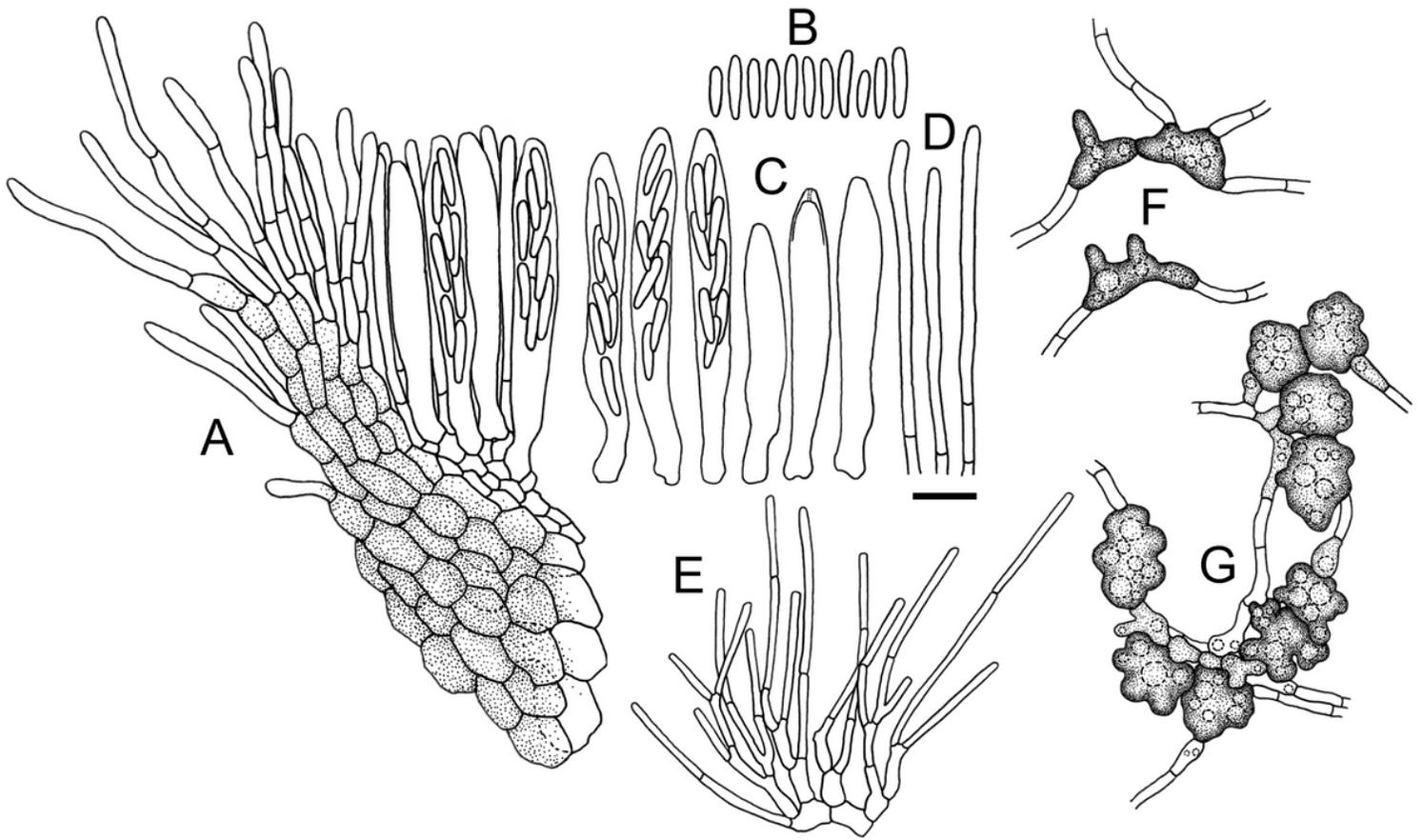
Figure 3

Line-drawings of *Cadophora fallopiae*. **A** vertical section of apothecia. **B** ascospores. **C** asci. **D** paraphysis. **E** conidiophores and conidia. **F** chlamydospore-like cells. **G** appressorium-like hyphal structures. Scale bar: 10 μm.
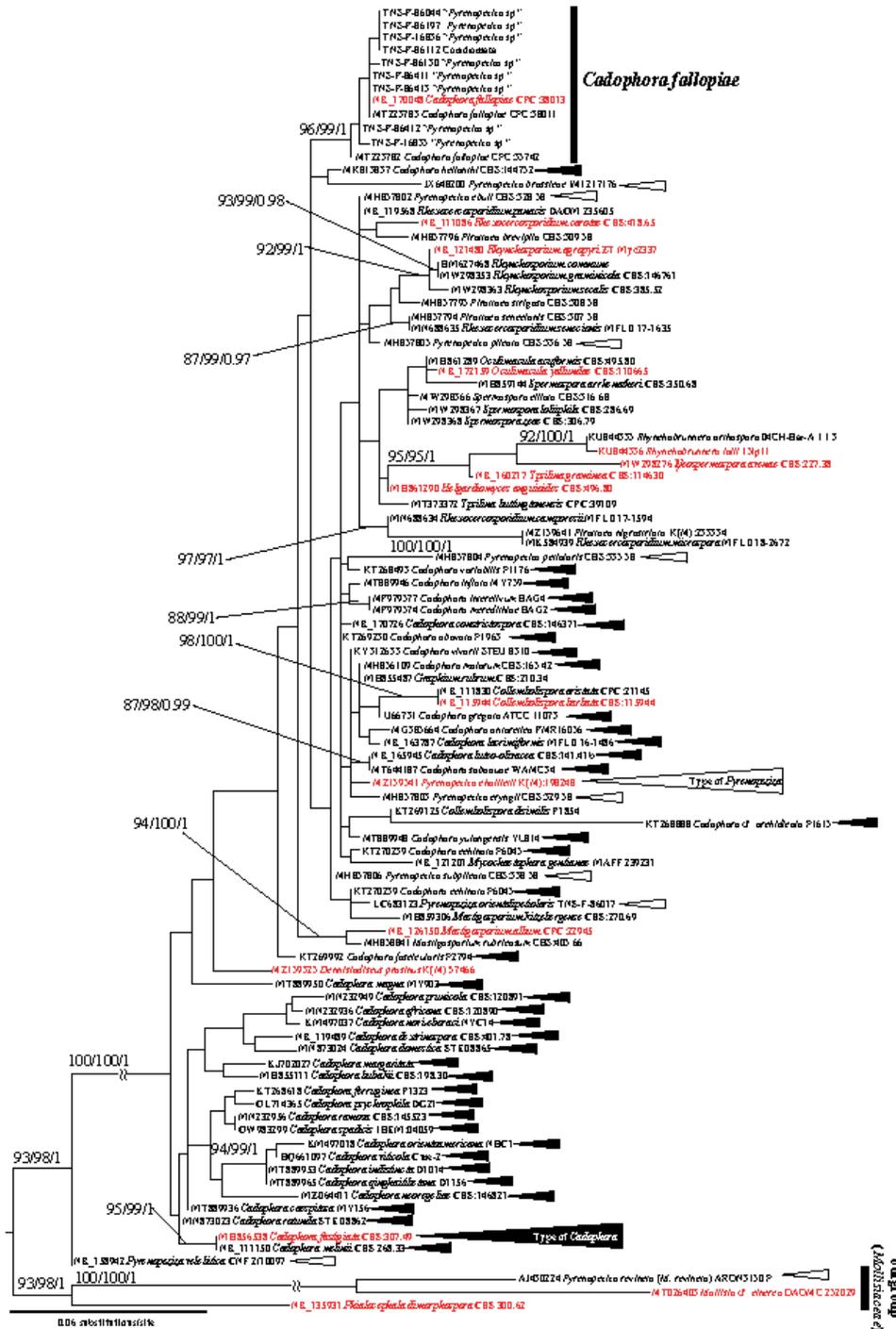
Figure 4

Maximum likelihood tree inferred from ITS sequences containing *Cadophora fallopiae* and its allies in *Pyrenopezizaceae*. Significant branch supported by SH-aLRT (≥80%)/ultrafast bootstrap (≥95%)/Bayesian posterior probabilities (≥0.95) are indicated. Type species are in red. GenBank and culture collection numbers are shown at the beginning and end of the species name, respectively (type

strains are in boldface). The tree is rooted with *Mollisia* cf. *cinerea* and *Phialocephala dimorphospora.* Black arrow points to *Cadophora*, and white arrow points to *Pyrenopeziza.*

Supplementary Files

This is a list of supplementary files associated with this preprint. Click to download.

- Table1.pdf
- Table2.pdf